Universiteit
Leiden
The Netherlands

Quantitative systems pharmacology modeling of biotherapeutics in oncology

Betts, A.M.

Citation

Betts, A. M. (2021, June 3). *Quantitative systems pharmacology modeling of biotherapeutics in oncology*. Retrieved from https://hdl.handle.net/1887/3176516

Version:	Publisher's Version
License:	Licence agreement concerning inclusion of doctoral thesis in the Institutional Repository of the University of Leiden
Downloaded from:	https://hdl.handle.net/1887/3176516

Note: To cite this publication please use the final published version (if applicable).

Cover Page

Universiteit Leiden

The handle http://hdl.handle.net/1887/3176516 holds various files of this Leiden University dissertation.

Author: Betts, A.M.
Title: Quantitative systems pharmacology modeling of biotherapeutics in oncology
Issue date: 2021-06-03

Chapter 5

Preclinical to Clinical Translation of Antibody-Drug Conjugates Using PK/PD Modeling:

A Retrospective Analysis of Inotuzumab Ozogamicin

Alison M. Betts, Nahor Haddish-Berhane, John Tolsma, Paul Jasper, Lindsay E. King, Yongliang Sun, Subramanyam Chakrapani, Boris Shor, Joseph Boni and Theodore R. Johnson

The AAPS Journal 18(5): 1101-1116 (2016)

5.1 Abstract

A mechanism-based pharmacokinetic/pharmacodynamic (PK/PD) model was used for preclinical to clinical translation of inotuzumab ozogamicin, a CD22-targeting antibody-drug conjugate (ADC) for B-cell malignancies including non-Hodgkin's lymphoma (NHL) and acute lymphocytic leukemia (ALL). Preclinical data was integrated in a PK/PD model which included: (1) a plasma PK model characterizing disposition and clearance of inotuzumab ozogamicin and its released payload N-Ac-γ-calicheamicin DMH, (2) a tumor disposition model describing ADC diffusion into the tumor extracellular environment, (3) a cellular model describing inotuzumab ozogamicin binding to CD22, internalization, intracellular N-Ac-γ-calicheamicin DMH release, binding to DNA or efflux from the tumor cell (4) tumor growth and inhibition in mouse xenograft models. The preclinical model was translated to the clinic by incorporating human PK for inotuzumab ozogamicin and clinically relevant tumor volumes, tumor growth rates and values for CD22 expression in the relevant patient populations. The resulting stochastic models predicted progression free survival (PFS) rates for inotuzumab ozogamicin in patients comparable to the observed clinical results. The model suggested that a fractionated dosing regimen is superior to a conventional dosing regimen for ALL, but not for NHL. Simulations indicated that tumor growth is a highly sensitive parameter and predictive of successful outcome. Inotuzumab ozogamicin PK and N-Ac-γ-calicheamicin DMH efflux are also sensitive parameters and would be considered more useful predictors of outcome than CD22 receptor expression. In summary, a multi-scale, mechanism-based model has been developed for inotuzumab ozogamicin, which can integrate preclinical biomeasures and PK/PD data to predict clinical response.

5.2 Introduction

Antibody-drug conjugates (ADCs) represent a promising therapeutic modality for clinical management of cancer (1, 2). There are more than 40 ADCs currently in different stages of clinical development for the treatment of various malignant diseases (3). In addition, brentuximab vedotin (Adcetris; Seattle Genetics) and ado-trastuzumab emtansine (T-DM1, Kadcyla; Roche-Genentech) are examples of recently approved ADCs on the market for oncology indications (2). ADCs currently in clinical development offer substantial improvements over first generation ADCs with more potent cytotoxins and superior conjugation stability (4). However, some ADCs are failing in the clinic due to insufficient efficacy (relative to standard of care) and off-target toxicity. For example, IMGN-901 is a CD-56-targeting ADC which failed to demonstrate sufficient improvement in efficacy over standard of care (etoposide/ carboplatin) in a Ph2 SCLC trial (5). Seattle Genetics discontinued the clinical development of vorsetuzumab mafodotin (SGN-75), an ADC for the treatment of solid tumors and hematological malignancies in favor of SGN-CD70A, an ADC against the same target but with a more potent payload (6). The timing is right to learn from these ADCs and to use the latest technology advancements to understand how they can be improved upon. Refinements in next generation ADCs are already being seen with advances in antibody engineering, improvements in linker-payload conjugation strategies (7) and the generation of novel highly potent payloads with different mechanisms of action (4, 8).

Mechanistic pharmacokinetic/pharmacodynamic (PK/PD) modeling is an example of an applied quantitative tool which can be used to provide understanding of the mechanistic processes of

drug action (9). The complex, non-linear processes involved in the physiological and cellular disposition of ADCs and their component parts make them ideal candidates for mechanistic modeling to enable integration and understanding of these multiple processes (10). The result is not only comprehension of the underlying system and mechanism of action, but also more tractable applications, including target feasibility, optimal ADC selection, preclinical to clinical translation and guidance on dose regimen optimization.

Quantitative modeling of ADCs in the literature to date has focused on empirical, data-driven PK/PD models (11, 12). These models are relatively easy to develop and apply and can be used for some level of extrapolation, e.g., across species (with some assumptions), to enable quantitative decision making. However, ADCs have intricate mechanisms of action, and the quantitative questions asked often require the use of more complex mechanistic models. For example, to optimize an ADC, properties of the target, including receptor expression, internalization rate and intracellular processing/recycling rate, need to be balanced (13). Properties of the ADC and its payload, including affinity for their targets and pharmacokinetics, also need to be included. While such models are an investment in terms of data requirements, they offer a high return of investment with respect to the granularity of the questions answered. Such a mechanistic PK/PD model for ADCs, capable of integrating preclinical biomeasures and PK/PD data to predict clinical response, was proposed by Shah, *et al.* (10). The authors used this model to quantitatively understand and characterize the disposition of brentuximab vedotin and its payload MMAE at the cellular and physiological level. A novel tumor penetration model was developed to predict intracellular tumor payload concentration, which was then linked to an optimized tumor growth inhibition model to characterize ADC efficacy in mouse xenograft models. The integrated mechanism-based PK/PD model was translated to the clinic and used to perform clinical trial simulation for brentuximab vedotin. The resulting multi-scale mechanistic modeling approach predicted progression free survival (PFS) rates and complete response rates for brentuximab vedotin in patients that were comparable to the observed clinical results. A different application of this model was described in a subsequent publication by Shah, *et al.* where it was used for a priori prediction of tumor concentrations of ADC and payload for an anti-5T4 ADC, A1mcMMAF (14). The model was also used to investigate sensitivity of model parameters. For example, payload dissociation from ADC and tumor size were found to be the most important determinants of plasma and tumor payload exposure.

In the analysis described herein, a mechanistic modeling approach was used to gain quantitative insight into the system dynamics of an anti-CD22 ADC in late stage clinical development for B-cell malignancies. Inotuzumab ozogamicin (CMC-544, PF-05208773) is an ADC composed of an IgG4 anti-CD22 monoclonal antibody conjugated to the enediyne DNA damaging agent N-Ac-γ-calicheamicin DMH via an acid-labile 4-(4'-acetylphenoxy)butanoic acid (Acbut) linker (15, 16). Inotuzumab ozogamicin is currently being evaluated in Phase 2/3 clinical trials for treatment of acute lymphoblastic leukemia (ALL). A Phase 3 study of inotuzumab ozogamicin in relapsed or refractory aggressive non-Hodgkin lymphoma (NHL) was discontinued due to lack of superiority relative to an active comparator arm (investigator's choice of bendamustine + rituximab or gemcitabine + rituximab) (17). Preclinically, inotuzumab ozogamicin inhibited the growth and establishment of B-cell lymphomas and induced the regression of disseminated B-cell lymphomas (Ramos, RL) and acute lymphoblastic leukemia (REH) in mouse xenograft models (15, 16). Mouse tumor growth inhibition data, along with inotuzumab ozogamicin plasma PK and target/system

parameters were used to perform mechanistic PK/PD modeling for inotuzumab ozogamicin and to predict intracellular tumor concentrations of N-Ac-γ-calicheamicin DMH. The model was translated to the clinic, and the results from simulated clinical trials were compared with observed clinical trial data to validate the translation process. The human model has subsequently been utilized for hypothesis generation and as a tool to answer mechanistic questions, including the effect of changes in antigen expression or efflux transporter capacity/status in patient tumors and the effect of changes in dose and/or regimen (in particular for ALL vs. NHL). This application of mechanistic PK/PD modeling demonstrates how preclinical data can be translated to the clinic to help scrutinize the mechanism of action of an ADC and predict outcome. Learnings can be applied to earlier stage programs as a quantitative tool to help guide their development.

5.3 Materials and Methods

CD22 Receptor Numbers

A quantitative flow cytometry method was developed to determine surface antibody binding capacity (ABC) per cell as a measure of receptor numbers using the parent antibody (G544) of inotuzumab ozogamicin conjugated 1:1 with phycoerythrin (PE) (18). Ramos and REH cell lines were cultured under standard culture conditions. A full binding curve was generated at 4°C under conditions that approached equilibrium to prevent internalization and samples were analyzed by FACS. The maximum specific binding fluorescent intensity derived from this data analysis was interpolated off a BD QuantiBRITE PE calibration curve to calculate the maximum ABC per cell as a measure of receptor numbers.

G544 Internalization

An imaging flow cytometry-based method was developed to measure internalization of G544, conjugated with PE or Alexa Fluor 647, under constant exposure condition. For each sample membrane and cytosolic intensity from CD22+ single cells were determined using area masks defined from the brightfield image of each cell. The extent of internalization at each time point was determined using IDEAS software internalization wizard which calculated an internalization score (IS) (19) based on the ratio of cytosolic intensity to total cell intensity using the upper quartile of pixel intensities. A plot of the IS vs. time was used to determine the initial half-life of internalization.

Binding Affinities

The binding of inotuzumab ozogamicin to CD22 receptors was evaluated using surface plasma resonance analysis, using the method of DiJoseph *et al.* (15), and the resulting K_d was determined to be 200 pM. The association rate constant (k_{on}) was assumed to be typical of monoclonal antibodies at approximately 5 x 10^5 $M^{-1}s^{-1}$ (20). The dissociation rate constant (k_{off}) was interpolated from the K_d and k_{on} using the relationship $K_d = k_{off} / k_{on}$ and was calculated to be 7.5 x 10^{-5} s^{-1}. As previously reported by Tianhu, *et al.*, N-Ac-γ-calicheamicin DMH binds to DNA with an estimated K_d of 135 nM (21).

Materials for Mouse Pharmacokinetic Study

Humanized IgG4 anti-CD22 antibody (G544) was provided by Celltech Chiroscience, plc, Wayne, PA. It was linked to calicheamicin with an acid labile AcBut (4-(4_acetylphenoxyl) butanoic acid) linker at Wyeth Research. Loading of calicheamicin onto the CD22 antibody was 50 μg of calicheamicin per mg of antibody and the average DAR was 3.5. The NHL B cell line RL (CRL-2261) was obtained from the American Type Culture Collection (ATCC, Manassas, VA). The cell line was determined to be mycoplasma free by a polymerase chain reaction mycoplasma detection assay. The cells were maintained as suspension cultures in RPMI medium plus 10% FCS, 10 mM HEPES, 1 mM sodium pyruvate, 0.2% glucose, Penicillin G sodium 100 U/mL, and streptomycin sulfate 100 μg/mL.

Mouse Pharmacokinetics

The PK of inotuzumab ozogamicin were determined following single intraperitoneal (IP) dose administration to non-tumor bearing female nude mice at 20 μg calicheamicin/kg (0.27 mg/kg inotuzumab) and 160 μg calicheamicin/kg (3.2 mg/kg inotuzumab), or to tumor (RL) bearing mice at 160 μg calicheamicin/kg (3.2 mg/kg inotuzumab) (Monolix software v3.2 (Lixoft, Antony, France)). Non-serial, terminal blood samples were collected by cardiac puncture under CO_2 anesthesia from 4 animals/group/time point at 0.1, 0.5, 1, 4, 8, 24, 48, 72, 96, 120, 168, 240 and 336 h post-dose. All blood samples were collected into tubes and stored on wet ice until the serum was separated by centrifugation at approximately 4°C for 15 min.

Assays to Quantify G544 (Total mAb) and Inotuzumab Ozogamicin (ADC)

Total mAb and ADC concentrations in mouse plasma were determined using a validated enzyme-linked immunosorbent assay (ELISA) with colorimetric detection. For the total mAb assay, the capture protein was a soluble form of recombinant CD22 protein (CD22:Fc fusion protein) and a monoclonal murine anti-human IgG4 conjugated to horseradish peroxidase (HRP) was used to detect bound G544, using 3,3',5,5'-tetramethylbenzidine (TMB) as the substrate for a colorimetric readout . For the ADC assay, CD22: Fc fusion protein was used to capture the G544 antibody portion of the ADC molecule. The calicheamicin portion of the molecule was then recognized with a rabbit anti-calicheamicin antibody. A goat anti-rabbit antibody conjugated to HRP was used to detect the bound rabbit antibody with TMB as the substrate for colorimetric readout.

Estimating Preclinical Pharmacokinetic Parameters for Total mAb, ADC and Payload Dissociation Rate

PK parameters for the mouse mAb were determined by fitting a 2-compartment PK model to the total mAb concentrations. It was assumed that the difference in clearance between the total mAb and ADC profiles was due to the dissociation of the calicheamicin payload (PL) from the mAb. The total mAb model with an additional clearance term describing dissociation of the PL was then fitted to the ADC concentration profile to estimate the dissociation rate constant, k_{dis}, *as* described previously (14).

Mouse Tumor Xenograft Studies

Tumor growth inhibition studies were completed in three different xenograft bearing mouse models: Ramos (Burkitt lymphoma), RL (non-Hodgkin's lymphoma) and REH (acute lymphoblastic leukemia), as reported in (15, 16). Briefly, female athymic nude mice were exposed to total body irradiation (400 rad) to suppress their residual immune system and facilitate the establishment of xenografts. Three days later, mice were injected subcutaneously with 5 x 10^6 REH ALL cells (6-8 mice/group) or 1 x 10^7 Ramos or RL cells (7-9 mice/group) suspended in Matrigel (Collaborative Biomedical Products, Belford, MA, USA, diluted 1:1 in RPMI-1640 medium) in the right flank for REH and left flank for RL and Ramos. Mice with staged tumors were administered normal saline (vehicle) or inotuzumab ozogamicin at Q4D x 3 regimen IP. Doses of inotuzumab ozogamicin were calculated based on quantity of N-Ac-γ-calicheamicin DMH AcBut and were 10, 40 and 160 µg calicheamicin/kg (0.14, 0.56, 2.22 mg/kg inotuzumab) for REH and Ramos or 20, 80 and 320 µg calicheamicin/kg (0.28, 1.11, 4.44 mg/kg inotuzumab) for RL. Tumors were measured at least once a week and their mass was defined as tumor volume (mm^3) = 0.5 × (tumor $width^2$) x (tumor length).

PK/PD Modeling

The mechanistic PK/PD model developed in this work and calibrated with the mouse xenograft data involved four major parts: 1) PK model describing time evolution of ADC and unconjugated payload in plasma, 2) tumor disposition model relating exposure between plasma and tumor, 3) cellular model describing intracellular payload at site of action, and 4) tumor growth and inhibition. This model is similar to the model developed and described previously (10), with main differences being a CD22 target in contrast to CD30 and calicheamicin payload (DNA toxin) in contrast to MMAE payload (tubulin inhibitor).

ADC and Unconjugated Payload PK

Plasma PK of inotuzumab ozogamicin and unconjugated payload (calicheamicin) after dose administration was modeled with a two-compartment IP model with additional terms characterizing the specific clearance into the tumor (JACOBIAN Modeling and Optimization Software, RES Group Inc., Needham, MA). The tumor disposition model is described in the subsequent section. The model equations are:

$$\frac{dA_0}{dt} = -k_a A_0$$

$$\frac{dA_1}{dt} = k_a A_0 + CLD\left(\frac{A_2}{V_2} - \frac{A_1}{V_1}\right) - CL\frac{A_1}{V_1} - \left(\frac{2P_{ADC}R_{cap}}{R_{krogh}^2} + \frac{6D_{ADC}}{R_{tumor}^2}\right)\left(\frac{A_1}{V_1} - \frac{Ab_f}{\epsilon}\right)\frac{w}{10^6}$$

$$\frac{dA_2}{dt} = CLD\left(\frac{A_1}{V_1} - \frac{A_2}{V_2}\right)$$

$$\frac{dPL_1}{dt} = k_{dis}DAR\frac{A_1}{V_{PL,1}} + CL\frac{A_1}{V_1}\frac{DAR}{V_{PL,1}} + CLD_{PL}\left(\frac{PL_2}{V_{PL,1}} - \frac{PL_1}{V_{PL,1}}\right) - CL_{PL}\frac{PL_1}{V_{PL,1}}$$
$$-\left(\frac{2P_{PL}R_{cap}}{R_{krogh}^2} + \frac{6D_{PL}}{R_{tumor}^2}\right)\left(PL_1 - \frac{PL_T}{\epsilon_{PL}}\right)\frac{w}{10^6}$$

$$\frac{dPL_2}{dt} = CLD_{PL}\left(\frac{PL_1}{V_{PL,2}} - \frac{PL_2}{V_{PL,2}}\right)$$

Parameter and variables for these equations are described in Tables 1 and 2.

Tumor Disposition Model

The tumor PK of ADC and unconjugated payload is described by a tumor disposition model (10, 22-24). Expressions describing transport into the tumor appear in the PK equations above and tumor compartment expression below as additional source and sink terms involving a number of additional parameters (e.g., $R_{cap}, R_{krogh}, P_{ADC}$, etc). Rather than estimating these parameters from the mouse xenograft data, values for permeability and diffusivity of the ADC and payload are determined from established correlations with molecular weight and known tumor size parameters (22-24). Values and references are provided in Table 2.

Tumor and Intracellular Concentrations and Dynamics

Concentrations of ADC and unconjugated payload in the tumor compartment and intracellular space are described by the equations below. The equations account for transport into the tumor compartment from plasma, binding and internalization into cell and binding of payload to the DNA target of calicheamicin.

$$\frac{dAb_f}{dt} = \left(\frac{2P_{ADC}R_{cap}}{R_{krogh}^2} + \frac{6D_{ADC}}{R_{tumor}^2}\right)\left(\frac{A_1}{V_1} - \frac{Ab_f}{\epsilon}\right) - k_{on}Ab_f\left(\frac{Ag - Ab_b}{\epsilon}\right) + k_{off}Ab_b$$

$$\frac{dAb_b}{dt} = k_{on}Ab_f\left(\frac{Ag - Ab_b}{\epsilon}\right) - k_{off}Ab_b - k_{int}Ab_b$$

$$\frac{dPL_T}{dt} = \left(\frac{2P_{PL}R_{cap}}{R_{krogh}^2} + \frac{6D_{PL}}{R_{tumor}^2}\right)\left(PL_1 - \frac{PL_T}{\epsilon_{PL}}\right) - k_{int}^{PL}PL_T + k_{out}^{PL}PL_{free}^{cell} + k_{dis}DAR\left(Ab_f + Ab_b\right)$$

$$\frac{dPL_{free}^{cell}}{dt} = k_{int}Ab_bDAR + k_{int}^{PL}PL_T - k_{out}^{PL}PL_{free}^{cell} - k_{on}^{PL}PL_{free}^{cell}\left(DNA - PL_b^{cell}\right) + k_{off}^{PL}PL_b^{cell}$$

$$\frac{dPL_b^{cell}}{dt} = k_{on}^{PL}PL_{free}^{cell}\left(DNA - PL_b^{cell}\right) - k_{off}^{PL}PL_b^{cell}$$

ADC and unconjugated payload enter the tumor compartment as described by the tumor disposition model. ADC binds with CD22 on the cell surface followed by internalization and

release of payload. Payload enters the cell via the ADC and also by non-specific internalization of unconjugated payload in the tumor compartment. Once inside the cell, payload can exit by exocytosis or remain in the cell and bind to the DNA target.

Tumor Growth and Inhibition

Tumor growth and inhibition is described using the Haddish-Berhane model (12), with equations shown below. Model variables are defined in Table 1.

$$\frac{dM_1}{dt} = \frac{k_{g0}\left(1-\frac{w}{M_{max}}\right)M_1}{\left(1+\left(\frac{k_{g0}}{k_g}w\right)^{\psi}\right)^{1/\psi}} - k_{max}\frac{PL_{total}^{\gamma}}{IC_{50}^{\gamma}+PL_{total}^{\gamma}}M_1$$

$$\frac{dM_2}{dt} = k_{max}\frac{PL_{total}^{\gamma}}{IC_{50}^{\gamma}+PL_{total}^{\gamma}}M_1 - \frac{M_2}{\tau}$$

$$\frac{dM_3}{dt} = \frac{M_2 - M_3}{\tau}$$

$$\frac{dM_4}{dt} = \frac{M_3 - M_4}{\tau}$$

The tumor growth portion of this model accounts for a preliminary exponential phase growth, followed by linear phase growth and a maximum tumor volume possible in the xenograft. Growth inhibition is modeled by a Hill equation as a function of intracellular payload concentration and several transduction compartments as cells are killed. The growth parameters are calibrated with data from the control arm of the mouse xenograft experiments and the drug-related death parameters are calibrated from the various dose arms.

Table 1: Model variables and terms used in equations

Variable	Definition	Unit
Ab_f, Ab_b	ADC concentration in tumor compartment, free and bound	nM
PL_T	Total free payload in cell	nM
$PL_{free}^{cell}, PL_b^{cell}$	Intracellular concentration of free and DNA-bound payload	nM
A_0, A_1, A_2	ADC dosed, central and peripheral compartments, respectively	nmol/kg
PL_1, PL_2	Concentration of free payload in central and peripheral compartments	nM
w	Tumor volume	mm^3
M_1, M_2, M_3, M_4	Tumor volume in growth and three transduction compartments	mm^3

Additional Equations

Several additional equations appear in the model, including tumor volume as a function of the transduction compartments, tumor mass radius (assuming spherical tumor), total intracellular payload and DAR as a function of dissociation rate.

$$w = M_1 + M_2 + M_3 + M_4$$

$$R_{tumor} = \left(\frac{3w}{4\pi}\right)^{1/3} \frac{1}{10}$$

$$PL_{total} = PL_T + PL_{free}^{cell} + PL_b^{cell}$$

$$\frac{dDAR}{dt} = -k_{dis} DAR$$

Calicheamicin Pharmacokinetics

Parameters for the plasma PK model of unconjugated calicheamicin are required for mouse to fit the xenograft tumor growth inhibition (TGI) data and for human for the subsequent clinical predictions. However, single dose IV data for calicheamicin was only available for rat and dog. A two compartment PK model was fit to this data to obtain values for $V_{PL,1}, V_{PL,2}, CL_{PL}$ and CLD_{PL} for both available species. PK parameter values for mouse and human were then obtained by allometric scaling the fitted rat and dog values. Note that the PK assay for unconjugated calicheamicin used a non-specific ELISA assay, which detects multiple forms of calicheamicin (i.e., N-Ac-γ-calicheamicin DMH + metabolites).

Clinical Pharmacokinetics of Inotuzumab ozogamicin

Clinical PK of inotuzumab ozogamicin is reported in two different Phase 1 studies in the literature (25, 26). Advani *et al.* describe a Phase 1 study of inotuzumab ozogamicin in an expanded MTD cohort of patients with relapsed or refractory CD22+ B-cell NHL (25). Ogura, *et al.* report a Phase 1 study of inotuzumab ozogamicin in Japanese patients with follicular lymphoma (FL) pre-treated with rituximab-based therapy (26). The PK was similar across both studies. For the modeling analysis herein, a simple 2-compartment model with linear elimination from the central compartment was used to characterize the PK of inotuzumab ozogamicin from Ogaru, *et al.* (26).

Preclinical to Clinical Translation

The integrated preclinical PK/PD model describing inotuzumab ozogamicin concentration-response relationship in REH, RL and Ramos xenograft bearing mice was translated to the clinic and used to perform clinical trial simulations. Three different types of CD22+ B-cell malignancies were considered in clinical trial simulations: follicular lymphoma (FL) and diffuse large B cell (DLBCL) subtypes of NHL and ALL. To enable preclinical to clinical translation the following changes were made to the model parameters: (a) relevant CD22 receptor expression levels for FL, DLBCL and ALL were included in the model (27), (b) initial tumor volumes and maximal

possible tumor volumes were changed to clinically observed/ plausible values (28, 29), and (c) growth rates for FL, DLBCL and ALL were set to clinically observed values (30-34). Clinical PK parameters for inotuzumab ozogamicin and calicheamicin were incorporated into the model as described above. The rest of the parameter values, including the inter-individual variability in PD parameters, were kept the same as the preclinical case. Preclinical PK/PD parameter estimates from RL/ Ramos cell lines were used to inform NHL clinical trial simulations, and REH cell line data was used for ALL clinical trial simulations. Please refer to Table 2 for the specific parameter values.

Clinical Trial Simulations

Clinical trial simulations for inotuzumab ozogamicin were performed using the parametric simulation method (JACOBIAN Modeling and Optimization Software, RES Group Inc., Needham, MA) (35). In each trial, 1,000 patients were simulated for each dose. For the NHL clinical trial simulations, the full PK/PD model was used including the parameters describing penetration of ADC into solid tumors (see Figure 1 and Table 2). Three different trials were simulated for NHL: patients with follicular lymphoma (FL), DLBCL patients (slow growth) and DLBCL patients (rapid growth). Two different tumor growth rates were considered for DLBCL to account for the large range in growth rates reported in the literature encompassing low-grade through to refractory aggressive B-cell NHL (30, 33)).

For the ALL clinical trial simulations the PK model was simplified by eliminating the parameters describing penetration into the solid tumor (Figure 1, red box). Instead rapid equilibrium between ADC in plasma and tumor interstitium was assumed, consistent with a liquid tumor. For both the NHL and ALL clinical trial simulations, two different dosing regimens were considered: 1.8 mg/m^2 (0.05mg/kg) Q4w x 3 and a fractionated regimen of 0.8, 0.5 and 0.5 mg/m^2 on day 1, 8 and 15 of a 28 day cycle, consistent with regimens explored in actual clinical trials for inotuzumab ozogamicin (25, 26, 36). In each case, the total dose administered was 1.8 mg/m^2.

For each simulated clinical trial, predicted tumor volumes were determined over time and PFS rates were calculated. For the NHL trials, these were compared to clinical trial data for inotuzumab ozogamicin (25). The criteria to categorize response rates for progressive disease, stable disease (SD), partial regression (PR), and complete regression (CR) for NHL were: more than 20% increase in tumor diameter, less than 30% reduction in tumor diameter, more than 30% decrease in tumor diameter but still detectable, and below the detection limit of 0.5 cm tumor diameter, respectively, according to the methods of Cheson, *et al.*(37). For hematological tumors like ALL, the criteria for SD, PR and CR were bone marrow blast cells >25%, 6-25% and < 5% respectively. CR with incomplete recovery (CRi) was defined as CR but without recovery of platelets to ≥ 100 × 10^9 / L or neutrophil counts to ≥ 10^9/L (36).

Table 2: Model parameters used in equations

	Parameter	Definition	Unit	Value (CV%)	Source
Preclinical Cellular Parameters	Ag	CD22 (antigen) concentration	nM	17.9$_{(Ramos)}$ 4.0$_{(RL)}$ 3.4$_{(REH)}$	Ramos/ REH: experimentally derived. RL from (27)
	k_{on}	Binding of antibody to CD22	1/nM/day,	43.2	Derived (20)
	k_{off}		1/day	6.48	(15)
	k_{int}	Internalization rate of bound antibody	1/day	199.6$_{(Ramos)}$ 199.6$_{(RL)}$ 199.6$_{(REH)}$	(38)
	k_{int}^{PL}	Internalization rate of free payload	1/day	9.66	Assumed same as MMAE
Preclinical Plasma PK Parameters	V_1	Volume of distribution in central compartment for ADC	L/kg	0.0478 (11)	Estimated from in-house mouse PK data
	V_2	Volume of distribution in peripheral compartment for ADC	L/kg	0.0214 (16)	
	CL	Plasma clearance of ADC	L/day/kg	0.039 (16)	
	CLD	Distribution clearance of ADC	L/day/kg	0.024 (-)	
	k_a	Absorption rate of ADC into central compartment	1/day	5.8 (37)	
	$V_{PL,1}$	Volume of distribution in central compartment for payload	L/kg	4.74	Extrapolated from in-house data
	$V_{PL,2}$	Volume of distribution in peripheral compartment for payload	L/kg	37.4	
	CL_{PL}	Plasma clearance of payload	L/day/kg	53.9	
	CLD_{PL}	Distribution clearance of payload	L/day/kg	31.8	
	k_{dis}	Dissociation rate of payload from ADC	1/day	0.24 (12)	Estimated from in-house data
	DAR	Drug-to-Antibody ratio	Unitless	3.5	Measured
Tumor Penetration Parameters	P_{ADC}, P_{PL}	Permeability of ADC and payload into tumor	µm/day	334, 18144	(22)
	D_{ADC}, D_{PL}	Diffusivity of ADC and payload into tumor	cm^2/day	0.022 0.125	(22)
	ϵ, ϵ_{PL}	Void fraction in tumor for ADC and payload	Unitless	0.24 0.44	(22)
	R_{cap}	Capillary radius	µm	8	(22)
	R_{krogh}	Average distance between 2 capillaries	µm	75	(22)
	R_{tumor}	Tumor radius	cm	Calculated	Assume spherical tumor

Preclinical PD Parameters	k_{g0}	Exponential tumor growth rate	1/day	0.08 (37)(REH) 0.122 (9)(RL) 0.211(16)(Ramos)	Estimated
	k_g	Linear tumor growth rate	mm^3/day	225 (43)(REH) 220 (-)(RL) 274 (27)(Ramos)	Estimated
	ψ	Switch between exponential and linear growth phases	Unitless	20	Fixed based on (39)
	M_{max}	Maximum tumor volume	mm^3	5000 (-)(REH), 6120 (82)(RL), 6160 (45)(Ramos)	Estimated
	k_{out}^{PL}	Exocytosis rate of intracellular payload	1/day	1.1 (57)	Estimated across models
	DNA	Concentration of DNA target in cell	nM	196 (60)	Estimated across models
	k_{max}	Maximum killing rate constant	1/day	17.6 (57)(REH), 14.0 (59)(RL), 15.6 (63)(Ramos)	Estimated
	IC_{50}	Concentration of payload corresponding to a killing rate constant of half maximum value	nM	399 (15)(REH), 237 (9)(RL), 227 (8)(Ramos)	Estimated
	γ	Hill coefficient of tumor killing function	Unitless	1	Fixed
	τ	Transduction time between tumor compartments	day	1.21 (14)(REH), 4.06 (52)(RL), 3.11 (75)(Ramos)	Estimated
Clinical PK Parameters	V_1	Volume of distribution in central compartment for ADC	L/kg	0.058 (11)	Derived from (26)
	V_2	Volume of distribution in peripheral compartment for ADC	L/kg	0.0124 (56)	
	CL	Plasma clearance of ADC	L/day/kg	0.029 (9)	
	$CLD,$	Distribution clearance of ADC	L/ day/kg	0.071 (135)	
	$V_{PL,1}$	Volume of distribution in central compartment for payload	L/kg	5.54	Extrapolated from in-house data
	$V_{PL,2}$	Volume of distribution in peripheral compartment for payload	L/kg	8.48	
	CL_{PL}	Plasma clearance of payload	L/day/kg	19.8	
	CLD_{PL}	Distribution clearance of payload	L/day/kg	114	
	k_{dis}	Dissociation rate of payload from ADC	1/day	0.47 (31)	Estimated from in-house data

	Ag	CD22 (antigen) concentration	nM	4.0(NHL:FL) 4.0(NHL:DLBCL) 0.09(ALL)	(27) Experimentally derived
	k_{g0}	Exponential tumor growth rate	1/day	0.012(FL) 0.02-0.05(DLBCL) 0.347(ALL, fast) 0.173(ALL,med) 0.120(ALL,slow)	(27-30)
Clinical PD Parameters	k_g	Linear tumor growth rate	mm^3/day	13,397	(34)
	$w0$	Initial tumor volume*	mm^3	>64cm^3 (76) >500cm^3 (30)(DLBCL) 1995 (1e9 cells) (ALL)	(32,33)

Sensitivity Analysis

A local sensitivity analysis was performed using the NHL clinical model to determine sensitivity of outcome (ORR) to variation in key model parameters. The parameters chosen were: exponential tumor growth rate (k_{g0}), CD22 receptor expression (Ag), calicheamicin efflux out of tumor cells ($k_{out,PL}$) and inotuzumab ozogamicin plasma clearance (CL). Nominal parameter values were k_{g0} = 0.012 day^{-1}, Ag = 8000 receptors/cell, $k_{out,PL}$ = 1.1 day^{-1}, CL = 29 mL/kg and initial tumor volume of 100 cm^3. Each parameter value was varied 10 fold in the sensitivity analysis, and model simulations used to calculate ORR according to the method of Cheson, *et al.* (37).

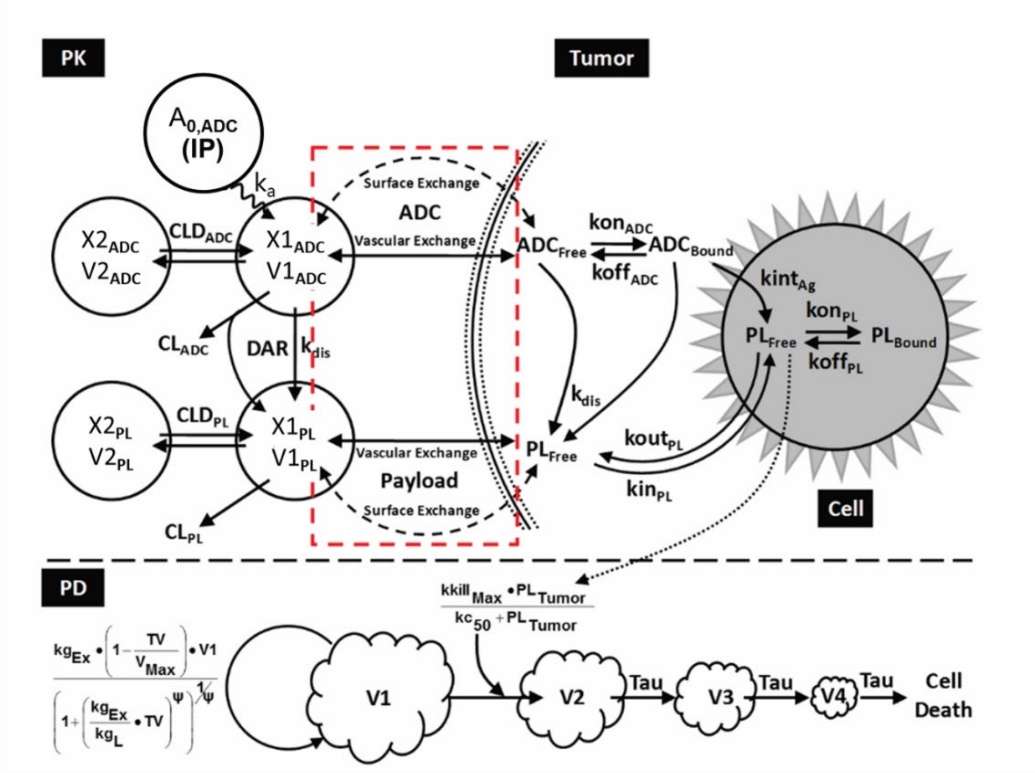

Figure 1: The PK/PD model for solid tumors (10). Note the model for liquid tumors (ALL) was approximated by eliminating transport to the solid tumor (shown in the red box). Please refer to the methods section and Tables 1 and 2 for detailed description of the symbols used in schematics.

5.4 Results

CD22 Receptor Expression and G544 Internalization

Anti-CD22 mAb (G544) binding capacity per cell was used as a measure of receptor number. G544 binding was saturable and minimal non-specific binding was observed for the cell lines tested. The receptor numbers for each cell line were determined from 3 separate independent experiments. On the Ramos NHL cell line there were 36,029 ± 5,004 CD22 receptors/cell, and on the ALL REH cells there were 5,037 ± 287 CD22 receptors/cell. These values were converted to nM for modeling purposes and are reported in Table 2. The internalization rate constant for G544 was found to be 199.6 day^{-1}, which corresponds to a half-life of internalization of 5 min (Table 2).

Mouse Pharmacokinetics

Determination of ADC PK Parameters

The plasma concentration-time profiles for inotuzumab ozogamicin obtained following single dose IP administration to non-tumor bearing mice at 20 μg calicheamicin/kg (0.27 mg/kg inotuzumab) and 160 μg calicheamicin/kg (3.2 mg/kg inotuzumab), or to tumor (RL) bearing mice at 160 μg calicheamicin/kg (3.2 mg /kg inotuzumab) are shown in Figure 2a. The data was dose proportional and concentrations were similar in both tumor bearing and non-tumor bearing mice. As a result, the data were pooled for parameter estimation. The estimated 2-compartment model parameters are provided in Table 2.

PK/PD Modeling of Mouse Xenograft Data

The characterization of mouse tumor growth inhibition data using the PK/PD model for Ramos, RL and REH bearing xenografts are shown in Figure 2b. The model was able to describe the observed data well and provided a set of PD parameters for preclinical to clinical translation of inotuzumab ozogamicin efficacy. Parameter estimates are provided in Table 2.

Determination of Calicheamicin PK Parameters

The pharmacokinetics of calicheamicin in mouse and human were obtained by allometric scaling of rat and dog data, available from in-house reports. The rat and dog PK parameters were estimated using a 2-compartment linear PK model. The calicheamicin mouse PK parameters were estimated by back extrapolation, and the human PK by forward extrapolation utilizing allometric principles (see Table 2 and Figure 3).

Clinical PK

A 2-compartmental linear PK model was used to characterize inotuzumab ozogamicin PK in clinical patients from Ogaru, *et al.* (26). The dissociation rate of calicheamicin in patients (k_{dis}) was determined by simultaneous fitting of the total Ab and ADC data, as described previously (*vide supra*). The estimated k_{dis} was 0.47 day^{-1} in patients. The estimated inotuzumab ozogamicin PK parameters utilized in the clinical trial simulations are presented in Table 2.

a.

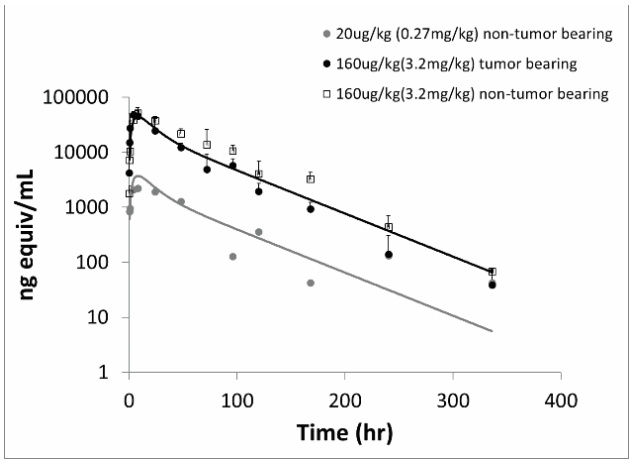

b.

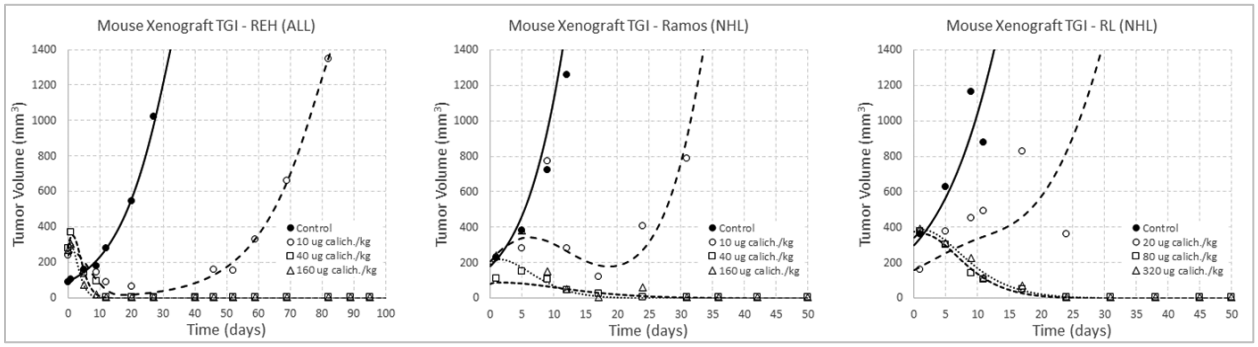

Figure 2a: Observed (*symbols*) and model fitted (*lines*) pharmacokinetics of inotuzumab ozogamicin in mouse plasma following single IP dose administration to non-tumor-bearing mice at 20 and 160 µg calicheamicin/kg (0.27 and 3.2 mg/kg inotuzumab, respectively) or to tumor (RL)-bearing mice at 160 µg calicheamicin/kg (3.2 mg/kg inotuzumab). **2b:** Observed (*symbols*) and model fitted (*lines*) tumor growth inhibition data in REH, Ramos and RL xenograft tumor-bearing mice following IP administration of inotuzumab Q4D × 3

Model Predictions of Tumor Calicheamicin Concentrations in NHL and ALL Cancer Patients

The model was used to simulate intracellular tumor calicheamicin concentrations in NHL (DLBCL) and ALL patient populations (see Figure 4). Following a single dose of inotuzumab ozogamicin at 1.8 mg/m^2, the concentrations of calicheamicin in the tumor were predicted to be significantly greater in ALL patients compared with NHL patients. This is consistent with greater diffusion/ accessibility of ADCs into liquid tumors (such as ALL) compared to solid tumors (such as NHL).

Use of the Model to Compare Tumor Volume Reductions in ALL Patients Following Different Dosing Regimens

The model was used to simulate reduction in tumor volume following different dosing regimens of inotuzumab ozogamicin. In Figure 5, four weekly administration of inotuzumab ozogamicin at 1.8 mg/m^2 and a weekly fractionated regimen of 0.8, 0.5 and 0.5 mg/m^2 are compared for ALL patients. The fractionated dosing regimen was predicted to be more efficacious than the Q4w regimen, sustaining tumor volume reduction for longer time periods.

Model Predictions of Clinical Outcome in NHL and ALL Cancer Patients

The model was used to simulate PFS times in NHL and ALL patient populations. The NHL clinical trial simulation was completed for FL and both slow and fast growing DLBCL patient populations using a regimen of inotuzumab ozogamicin given every 4 weeks, to mimic treatment in the Advani clinical trial (25). Figure 6 compares the model simulated and observed PFS data, which were found to correlate well. PFS rates were also predicted for ALL following a fractionated regimen (0.8, 0.5 and 0.5 mg/m^2 on days 1, 8 and 15 of a 28 day cycle), but could not be compared with clinical observations as studies are still under completion and PFS data is not available yet. However, the model predictions for complete response (CR) of 60-79% using two different growth rates for ALL, compare favorably with CR/CRi of 80.7% (72-88) demonstrated by inotuzumab ozogamicin in an ongoing phase 3 study in patients with ALL (40).

Sensitivity Analysis

Sensitivity of variation in exponential tumor growth rate (k_{g0}), CD22 receptor expression (Ag), calicheamicin efflux out of tumor cells ($k_{out,PL}$) and inotuzumab plasma clearance (CL) on inotuzumab ORR was examined in the NHL (FL) model. The plots in Figure 7 show how ORR varies over a dose range from 0 to 0.06mg/kg (2.16mg/m^2) with a 10- fold change in each parameter from its nominal value. The cross hairs on the plots represent the nominal case for Inotuzumab given at its recommended dose of 0.05mg/kg (1.8mg/m^2). The most sensitive parameter was tumor growth rate, followed by PL efflux and then Inotuzumab clearance. CD22 expression was the least sensitive parameter.

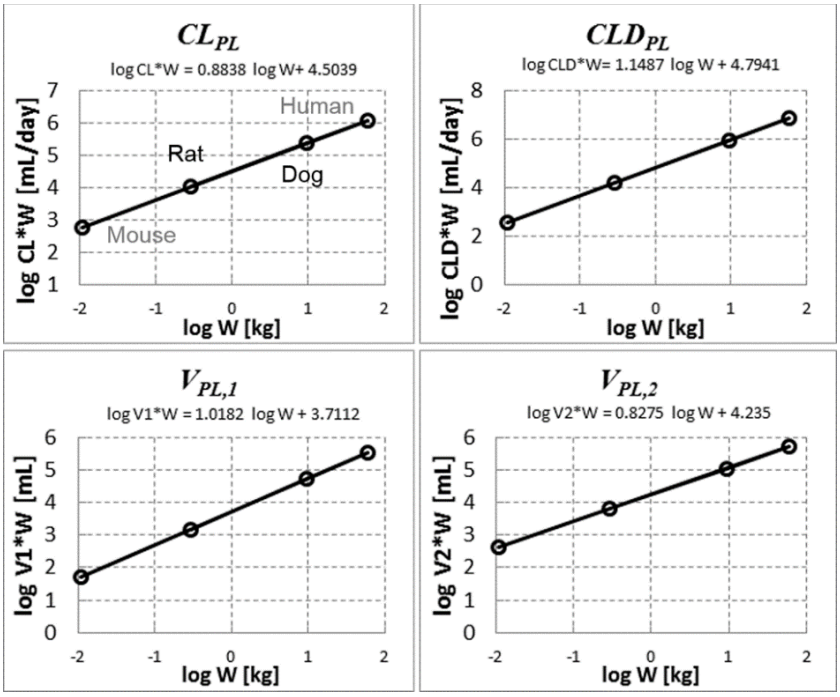

Figure 3: Allometric scaling of calicheamicin PK from rat and dog to human and mouse. In this context, *W* refers to body weight.

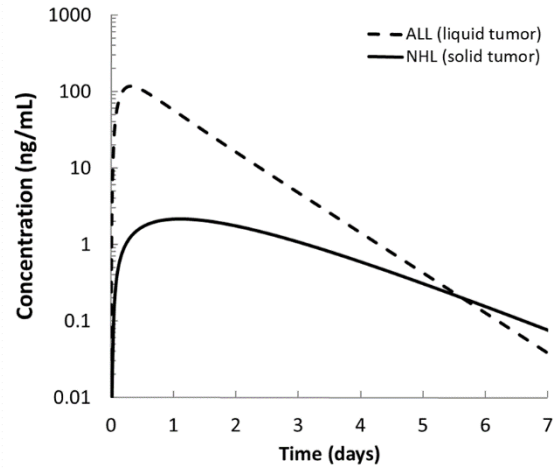

Figure 4: Model predicted intracellular calicheamicin PK for ALL (liquid tumor) and NHL (solid tumor).

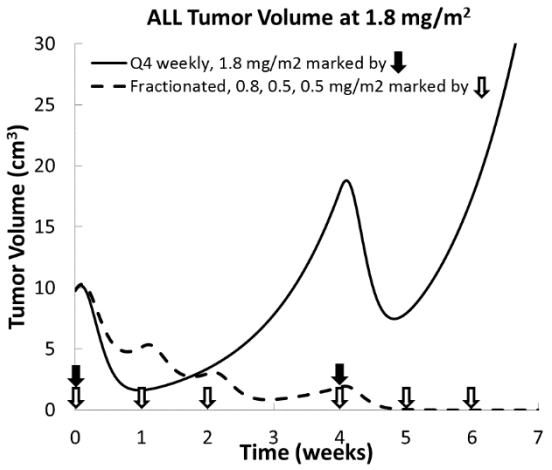

Figure 5: Simulated tumor volume profiles over time for a Q4 weekly dosing regimen and a fractionated Q1 weekly regimen for ALL patients receiving a total dose of inotuzumab ozogamicin of 1.8 mg/m^2

5.5 Discussion

Challenges in Predicting Clinical Efficacy of Anti-Cancer Agents from Preclinical Data

Prior knowledge of the expected efficacious dose of an oncology drug in the clinic is desirable for optimal design of clinical trials to ensure that an efficacious dose can be reached with acceptable toxicity profile. However, predicting efficacy of anti-cancer agents in the clinic remains a challenge. A problematic issue is that the preclinical tools used for identification of clinical drug candidates, such as mouse xenograft models, are thought to be poorly predictive of the clinical outcome (41-44). At a minimum, differences between preclinical and clinical drug exposures should be factored into clinical predictions. Indeed analyses by Rochetti *et al.* and Wong *et al.* showed that incorporation of human PK into xenograft data significantly improved quantitative prediction (43, 45).

ADCs offer an additional level of complexity, as they are composed of multiple entities including an antibody, linker, and payload, which could potentially be responsible for driving efficacy and toxicity (46). The accuracy of the exposure response characterization and translation to the clinic will depend upon the exposure endpoint chosen. Typically, the concentration of drug in the plasma or blood is the preferred exposure endpoint to correlate with efficacy, as it is both an easily accessible biological sample and for many small molecule drugs it correlates well with drug concentration at the site of action. However, for large molecules such as antibodies and ADCs, the concentration in the plasma does not represent concentration in the solid tumor due to a complex biodistribution mechanism. Optimal translation requires use of drug concentration in the tumor as the exposure endpoint to accurately determine the exposure response relationship. Measurement of drug in the tumor is a costly, labor intensive process which may not be feasible and presents another challenge. For ADCs, it is necessary to determine the concentration of the released payload following ADC administration, as this concentration is responsible for eliciting the pharmacological action.

Given the challenges of trying to predict efficacy using mouse xenografts, which are an imperfect representation of human tumors, and the complexity of determining the relevant exposure endpoint (tumor payload concentration), it is not surprising that predicting efficacy of ADCs in the clinic is problematic. When dealing with complex biological systems with multiple variables and pathways, it is advisable to build a mathematical model of the system, capable of integrating and interpreting preclinical data and providing a quantitative framework for translation to the clinic (9, 47).

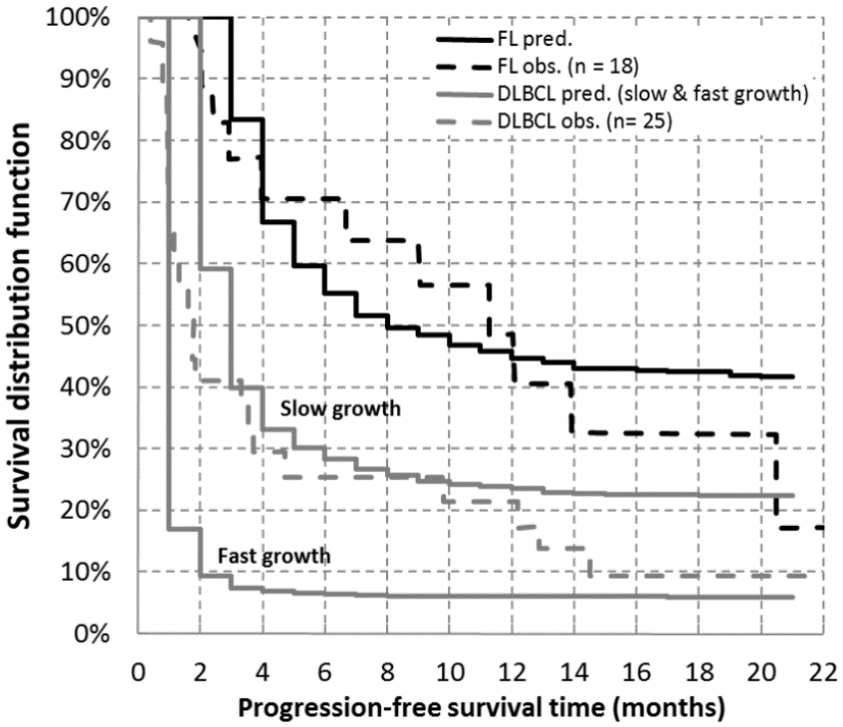

Figure 6: Model predicted PFS rates in NHL patients from Clinical Trial Simulations and Comparison with Clinical Trial Results. The solid lines represent model simulated PFS rates after dosing inotuzumab ozogamicin at 1.8 mg/m^2 every 4 weeks to NHL patients. The dashed lines represent observed PFS rates in patients administered the same dose and regimen in clinical trials. Note, clinical trial simulations were completed for FL and both slow and fast growing DLBCL patient populations, to be consistent with treatment in clinical trials.

Tumor Cell Processing of Inotuzumab ozogamicin

In this work, we have taken inotuzumab ozogamicin (CMC-544), which is an anti-CD22 ADC in the clinic for both solid tumor (NHL) and hematological malignancies (ALL) (48), and used a systems pharmacology modeling approach to investigate translation from pre-clinical data to the clinic. The model used was based on a mechanism-based, multiscale ADC PK/PD model proposed by Shah *et al.,* capable of integrating preclinical biomeasures and PK/PD data to predict clinical response (10). Shah and colleagues used this model for a 'bench to bedside' translation of brentuximab vedotin and demonstrated its ability to predict clinical responses for this ADC. In

the analysis herein, we applied the same type of approach for inotuzumab ozogamicin to gain quantitative insight into the mechanism of action of this ADC.

The modeling process starts with a rigorous understanding of the mechanism of action of inotuzumab ozogamicin at the cellular level to build a model which represents the disposition of the ADC and release of payload in the tumor cell. Once in the extracellular tumor environment, inotuzumab ozogamicin binds to its target CD22 on the surface of tumor cells and is rapidly internalized by receptor mediated endocytosis. The ADC is trafficked intracellularly from the endosomes to the lysosomes. The AcBut-hydrazone linker, which tethers the CD22 mAb to the payload calicheamicin, is acid labile and is cleaved in the lysosomes to release the payload. The liberated N-Ac-γ-calicheamicin DMH payload is subsequently released into the cytosol where it is reduced by glutathione to form the reactive diradical form. This activated form of calicheamicin distributes to the nucleus where it binds to the minor groove in DNA and causes double-strand breaks, resulting in cell death (48). Alternatively, the released payload form, N-Ac-γ-calicheamicin DMH, can also bind to P-glycoprotein (P-gp) prior to nuclear translocation and be effluxed from the cell (49).

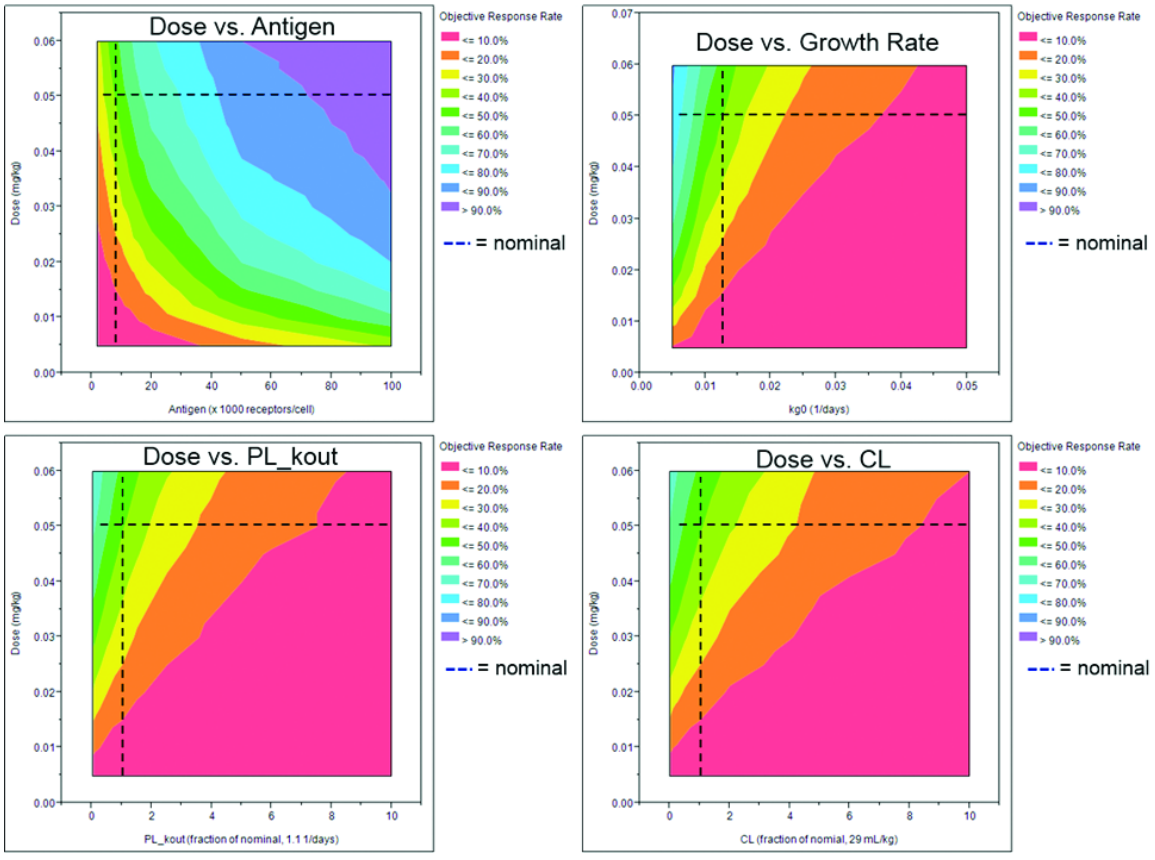

Figure 7: Local Parameter Sensitivity Analysis. Sensitivity of outcome (ORR) to variation in CD22 antigen concentration (*Ag*), exponential tumor growth rate (k_{g0}), calicheamicin efflux (*PL_kout*) and inotuzumab ozogamicin clearance (CL) was examined in the NHL (FL) model. Nominal parameter values were *Ag* = 8000 receptors/cell, k_{g0} = 0.012 day^{-1}, *PL_kout* = 1.1 day^{-1}, CL = 29 mL/kg and initial tumor volume of 100 cm^3. The cross hairs on the plots represent the nominal case for Inotuzumab given at its recommended dose of 0.05mg/kg (1.8mg/m^2).

In building the tumor cell component of the PK/PD model, the goal was to provide a quantitative description of the principal operative intracellular processes. The first step was to determine which parameters were available from the literature and which were considered important enough to warrant experimental work to inform the model. From previous analyses, key cellular parameters governing the success of an ADC include antibody affinity to its receptor, receptor expression levels and internalization rate into the tumor cell (13, 14, 50). Payload affinity for its target and efflux of payload out of the cell are also key parameters in establishing payload concentration and retention in the cell (10). For this analysis, binding affinity data for antibody to CD22 (15) and calicheamicin to DNA (21), were available from the literature and could be incorporated directly into the model. Internalization rates and CD22 receptor expression were not available for all relevant cell lines and were therefore determined in-house.

The parameter k_{out} describes the exocytosis rate of N-Ac-γ-calicheamicin DMH from the tumor cell, incorporating active processes such as efflux by P-glycoprotein (P-gp). This is important as **P-**gp is upregulated on many tumor cell types. Data to inform k_{out} was not available in the literature and a method was not available to determine this experimentally. Instead k_{out} was estimated within the model. The value of k_{out} estimated for calicheamicin in the model (1.1 day^{-1}; Table 2) was very similar to values used for monomethylauristatin E (MMAE; 0.68-1.1 day^{-1}) in a similar modeling application (10). This makes some sense, as calicheamicin and MMAE are ADC payloads which are both reported to be substrates for P-gp (49, 51). Experimental data would have been optimal to inform the k_{out} parameter for calicheamicin, but in absence of this data the estimated value is in line with a similar ADC payload.

Tumor Growth Inhibition in Mouse as a Function of Tumor Calicheamicin Concentrations

The next step was to combine the tumor cell component with a PK model describing the disposition/ elimination of ADC and payload in the plasma and distribution to the tumor cell. The plasma PK model structure describes distribution of inotuzumab ozogamicin into peripheral tissues, and ADC catabolism and de-conjugation to release payload into the systemic circulation. The entire payload released systemically from the hydrolysis of the acid-labile hydrazone linker was assumed to be N-Ac-γ-calicheamicin DMH. It is possible that metabolites are also formed which were not specified in the model. However, since the unconjugated calicheamicin PK assay used a non-specific ELISA method, it may well detect some of these calicheamicin metabolites. The model also accounts for distribution and clearance of the payload. Important data to characterize this part of the model included inotuzumab ozogamicin PK in mouse (total antibody and ADC) and calicheamicin PK. The plasma concentrations of ADC and payload were characterized using a simple two compartmental model. This step also enabled estimation of the rate of dissociation of payload from the ADC (k_{dis}), providing an estimate of the drug to antibody ratio (DAR) for ADCs that would internalize into cancer cells.

The solid tumor penetration part of the model was incorporated using drug exchange parameters from the literature (10, 22, 52, 53). The model assumes that diffusion is the predominant pathway of ADC passage into the tumor, as the high interstitial pressure within the tumor and absence of lymphatics means that convection is absent or minimal. The drug exchange parameters account for the size of the molecule being exchanged, the vascular permeability, tissue diffusion rates and accessible tissue volume corresponding to that size. The model includes diffusion from the

periphery of the tumor which is predominant when the tumors are small and avascular. As the tumor becomes larger, diffusion from the vasculature takes over as the dominant pathway (10, 22, 52, 53). Once the ADC is in the tumor interstitium, the cellular model is used to describe binding to the target and intracellular processing and binding.

The advantage of using a physiological relevant PK model for inotuzumab ozogamicin was that it enabled prediction of tumor calicheamicin concentrations, which are a more appropriate exposure endpoint to link to tumor regression/efficacy. The efficacy of inotuzumab ozogamicin was studied in 3 different xenograft bearing mouse models: Ramos (Burkitts lymphoma), RL (NHL) and REH (ALL) (15, 16). The mechanism-based tumor disposition model was combined with a pharmacodynamic model of tumor growth and cell kill (12), in which tumor payload concentrations were used to drive efficacy. The model features a dynamic interaction between tumor distribution parameters and tumor size, where changes in tumor volume are directly able to influence the concentration of payload in the tumor, which in turn is responsible for the size of the tumor. As shown in Fig. 2b, the PK/PD model was able to provide a good fit to the observed inotuzumab ozogamicin preclinical TGI data, providing estimates of the efficacy parameters and the inter-individual variability associated with them.

Translation to the Clinic

Once the preclinical PK/PD relationship describing tumor growth inhibition as a function of tumor calicheamicin concentration had been characterized, the next step was to translate this model to the clinic to predict inotuzumab ozogamicin efficacy in patients. The overall model structure was kept the same, with the exception that mouse system parameters such as initial tumor size, tumor growth rates and receptor expression were replaced with clinically relevant parameters, to make the model representative of the human system. In addition, inotuzumab ozogamicin and calicheamicin clinical PK were incorporated into the model. To accomplish this, a two compartment linear PK model was used to fit the Phase 1 clinical PK data for inotuzumab ozogamicin (26). Clinical PK for calicheamicin was allometrically scaled from rat and dog (Figure 3). The rate of dissociation of payload from the ADC (k_{dis}) was determined in clinical data by simultaneous fitting of the total mAb and ADC data. Since the parameters describing the tumor disposition are clinically translatable, they were kept the same (10). In addition, drug specific parameters including binding parameters for ADC and calicheamicin to their targets, internalization rate, exocytosis rate of intracellular payload (k_{outPL}), IC_{50}, kill rate (k_{max}) and transduction time between tumor compartments (τ) were not changed. Most importantly, systems parameters were changed to match literature estimates for NHL and ALL patients. For example, initial tumor volumes for NHL and ALL were taken from the literature (28, 29). Tumor growth rates and CD22 receptor expression for low grade NHL (FL), refractory aggressive NHL (DLBCL) and ALL were all used in clinical simulations (27, 30-34).

This 'switching' of systems parameters from murine values to relevant clinical values for the disease population gives this method for translating efficacy a greater level of relevance and fidelity compared to previous translational approaches which account for exposure differences only (43, 45). Following translation of the PK/PD model to the clinic, the model was used to perform clinical trial simulations.

Simulations of Tumor Calicheamicin Concentrations

In the first simulations, tumor concentrations of calicheamicin in NHL (DLBCL) and ALL patient populations were compared following equivalent doses of inotuzumab ozogamicin (1.8mg/m^2 Q4w) to each group. The PK model for NHL (DLBCL) differed from the ALL model in terms of the tumor penetration parameters. NHL is considered to be a malignant solid tumor of the immune system which can arise from undifferentiated lymphoid cells in virtually any part of the body. Drug exchange parameters for solid tumors are therefore required to describe penetration of inotuzumab ozogamicin into the NHL tumor types. In contrast, ALL is a hematopoietic or 'liquid' tumor which arises in the bone marrow. These tumors have less of a barrier to diffusion compared with solid tumors. As a result, the PK/PD model was simplified by elimination of the drug exchange tumor penetration parameters, and equilibrium was assumed between ADC concentration in plasma and tumor interstitium. The manifestation of the difference in the tumor model between a liquid tumor (such as ALL) and a solid tumor (such as DLBCL) is shown in Figure 4. Following the same dose of inotuzumab ozogamicin, the ALL tumor calicheamicin concentrations are predicted to be approximately 2 orders of magnitude higher than the DLBCL tumor calicheamicin concentrations. This simulation suggests that liquid tumors such as ALL will be easier to treat, requiring lower doses than solid tumors. This simulation agrees with the observation that solid tumors are often difficult for drugs to penetrate (54).

Simulations of Optimal Dosing Regimens for ALL

The model was also used to simulate different dosing regimens for treating ALL. The first regimen selected was 1.8mg/m^2 Q4w, which had been investigated in clinical trials for inotuzumab ozogamicin in the treatment of NHL (25). The second regimen was a fractionated schedule of 3 weekly doses over a 4-week treatment cycle, with doses of 0.8, 0.5, and 0.5mg/m^2 on days 1, 8 and 15 respectively. This regimen is under investigation in clinical trials for the treatment of ALL (40). Both regimens had the same total dose of 1.8mg/m^2 per monthly cycle. Individual subject tumor volume plots over time are shown in Figure 5 (with the subject chosen having median rate of clearance of inotuzumab ozogamicin). In the ALL simulations, the fractionated dosing regimen was predicted to be more tumor regressive than the Q4 weekly regimen. Although Q4 weekly dosing results in higher tumor suppression at each dose, this is offset by considerable tumor re-growth. In contrast, the fractionated dosing results in a more constant suppression over the dosing period. This analysis demonstrates that prediction of optimal dosing regimen is dependent on integration of all parameters and is therefore a worthy application of this type of mechanistic model.

Prediction of Progression Free Survival Rates

For each simulated clinical trial, PFS rates were calculated (Figure 6). For the NHL trial, PFS predictions could be compared with clinical trial data for inotuzumab ozogamicin (25). For both FL and DLBCL, the model predicted PFS and observed data from clinical trial compared well. Interestingly, large drops in PFS were observed at the longest survival times in the clinical trial, which may have been due to the small 'n' number by this stage of the analysis. In contrast, the model predicts a more logical flattening of PFS at the longer survival times.

Sensitivity Analysis

The final application of the model in this analysis was to perform a local sensitivity analysis to give insight into the most important parameters defining, or even limiting, efficacy of inotuzumab ozogamicin versus NHL. CD22 receptor expression, calicheamicin efflux rate, inotuzumab ozogamicin PK (clearance rate) and tumor growth rate were selected as interesting parameters to vary in the model. The impact of varying these parameters over orders of magnitude from their nominal values, at a range of inotuzumab ozogamicin doses, is shown in Figure 7. At the recommended dose of 1.8 mg/m^2 (0.05 mg/kg) the least sensitive parameter was CD22 receptor expression, indicating that for inotuzumab ozogamicin this is least limiting for efficacy and probably reflects the optimal characteristics of this receptor as an ADC target, due to its high expression across B-cell types and rapid internalization (and recycling rates). Calicheamicin efflux from the tumor cell was a more sensitive parameter, indicating the impact of this parameter on intracellular payload concentrations and resultant efficacy. This is important, as N-Ac-γ-calicheamicin DMH is known to be a substrate for P-glycoprotein (P-gp), an efflux transporter which is upregulated on many tumor cell types (49). A further development of the model would be to include P-gp expression across cell lines or patients to investigate its relationship with efflux. Data was not available to support this in the current version of the model; however, this refinement would enable assessment of MDR1 as a quantitative diagnostic of efficacy.

Clearance was also a sensitive parameter for inotuzumab ozogamicin. Compared to more recent ADCs, inotuzumab ozogamicin has a faster rate of clearance, likely due to the contribution of CD22 receptor-mediated clearance as an additional CL mechanism, supplemental to the usual mechanisms of ADC catabolism and de-conjugation. As can be seen from the sensitivity plots, high clearance values of inotuzumab ozogamicin have a substantial impact on efficacy. However, the most sensitive parameter was rate of tumor growth in the model, indicating that even at nominal clearance and efflux values, the most aggressive, refractory tumors require higher doses for treatment of NHL.

5.6 Conclusions

In summary, a mechanism-based PK/PD model has been used for preclinical to clinical translation of inotuzumab ozogamicin. The model was able to predict PFS responses for inotuzumab versus NHL that were comparable to observed clinical trial results, demonstrating its utility for predicting efficacy of ADCs. The model was also able to give useful mechanistic insight into optimal dosing regimens and sensitive parameters impacting outcome, including tumor growth rate, inotuzumab ozogamicin clearance and calicheamicin efflux. This knowledge could be applied to optimize the design of ADCs in the discovery phase of research, and/or for selection of predictive diagnostics in the clinic.

References

1. Webb, S. Pharma interest surges in antibody drug conjugates. *Nature biotechnology* **29**, 297-8 (2011).
2. Zolot, R.S., Basu, S. & Million, R.P. Antibody-drug conjugates. *Nature reviews Drug discovery* **12**, 259-60 (2013).

3. Sohayla Rostami, I.Q., Robert Sikorski. *The Clinical Landscape of Antibody-drug Conjugates*. (2014).
4. Mack, F., Ritchie, M. & Sapra, P. The next generation of antibody drug conjugates. *Seminars in oncology* **41**, 637-52 (2014).
5. *ImmunoGen, Inc. Announces Discontinuation of IMGN901 Study in Small-Cell Lung Cancer (SCLC)*. (2013).
6. Williams, R. Discontinued in 2013: oncology drugs. *Expert opinion on investigational drugs* **24**, 95-110 (2015).
7. Panowksi, S., Bhakta, S., Raab, H., Polakis, P. & Junutula, J.R. Site-specific antibody drug conjugates for cancer therapy. *mAbs* **6**, 34-45 (2014).
8. Maderna, A. *et al.* Discovery of cytotoxic dolastatin 10 analogues with N-terminal modifications. *Journal of medicinal chemistry* **57**, 10527-43 (2014).
9. Agoram, B.M., Martin, S.W. & van der Graaf, P.H. The role of mechanism-based pharmacokinetic-pharmacodynamic (PK-PD) modelling in translational research of biologics. *Drug Discov Today* **12**, 1018-24 (2007).
10. Shah, D.K., Haddish-Berhane, N. & Betts, A. Bench to bedside translation of antibody drug conjugates using a multiscale mechanistic PK/PD model: a case study with brentuximab-vedotin. *Journal of pharmacokinetics and pharmacodynamics* **39**, 643-59 (2012).
11. Jumbe, N.L. *et al.* Modeling the efficacy of trastuzumab-DM1, an antibody drug conjugate, in mice. *Journal of pharmacokinetics and pharmacodynamics* **37**, 221-42 (2010).
12. Haddish-Berhane, N. *et al.* On translation of antibody drug conjugates efficacy from mouse experimental tumors to the clinic: a PK/PD approach. *Journal of pharmacokinetics and pharmacodynamics* **40**, 557-71 (2013).
13. Sadekar, S., Figueroa, I. & Tabrizi, M. Antibody Drug Conjugates: Application of Quantitative Pharmacology in Modality Design and Target Selection. *The AAPS journal* **17**, 828-36 (2015).
14. Shah, D.K. *et al.* A priori prediction of tumor payload concentrations: preclinical case study with an auristatin-based anti-5T4 antibody-drug conjugate. *The AAPS journal* **16**, 452-63 (2014).
15. DiJoseph, J.F. *et al.* Antibody-targeted chemotherapy with CMC-544: a CD22-targeted immunoconjugate of calicheamicin for the treatment of B-lymphoid malignancies. *Blood* **103**, 1807-14 (2004).
16. Dijoseph, J.F., Dougher, M.M., Armellino, D.C., Evans, D.Y. & Damle, N.K. Therapeutic potential of CD22-specific antibody-targeted chemotherapy using inotuzumab ozogamicin (CMC-544) for the treatment of acute lymphoblastic leukemia. *Leukemia* **21**, 2240-5 (2007).
17. *Pfizer Discontinues Phase 3 Study of Inotuzumab Ozogamicin in Relapsed or Refractory Aggressive Non-Hodgkin Lymphoma (NHL) Due to Futility* (2013). Accessed May 20th 2013.
18. Wang, L., Abbasi, F., Gaigalas, A.K., Hoffman, R.A., Flagler, D. & Marti, G.E. Discrepancy in measuring CD4 expression on T-lymphocytes using fluorescein conjugates in comparison with unimolar CD4-phycoerythrin conjugates. *Cytometry Part B, Clinical cytometry* **72**, 442-9 (2007).
19. Sherree Friend, T.G., Brian Hall, Vidya Venkatachalam, Philip Morrissey. *Intracellular localization and trafficking using the ImageStream® imaging flow cytometer*.
20. Poulsen, T.R., Jensen, A., Haurum, J.S. & Andersen, P.S. Limits for antibody affinity maturation andrepertoire diversification in hypervaccinated humans. *Journal of immunology* **187**, 4229-35 (2011).
21. Tianhu Li, Z.Z., Virginia A. Estevez, Kai U. Baldenius, K. C. Nicolaou, and Gerald F. Joyce. Carbohydrate-Minor Groove Interactions in the Binding of Calicheamicin γ1 to Duplex DNA. *J Am Chem Soc* **116**, 3709-15 (1994).
22. Schmidt, M.M. & Wittrup, K.D. A modeling analysis of the effects of molecular size and binding affinity on tumor targeting. *Molecular cancer therapeutics* **8**, 2861-71 (2009).

23. Thurber, G.M., Schmidt, M.M. & Wittrup, K.D. Antibody tumor penetration: transport opposed by systemic and antigen-mediated clearance. *Adv Drug Deliv Rev* **60**, 1421-34 (2008).
24. Thurber, G.M., Schmidt, M.M. & Wittrup, K.D. Factors determining antibody distribution in tumors. *Trends in pharmacological sciences* **29**, 57-61 (2008).
25. Advani, A. *et al.* Safety, pharmacokinetics, and preliminary clinical activity of inotuzumab ozogamicin, a novel immunoconjugate for the treatment of B-cell non-Hodgkin's lymphoma: results of a phase I study. *Journal of clinical oncology : official journal of the American Society of Clinical Oncology* **28**, 2085-93 (2010).
26. Ogura, M. *et al.* Phase I study of inotuzumab ozogamicin (CMC-544) in Japanese patients with follicular lymphoma pretreated with rituximab-based therapy. *Cancer science* **101**, 1840-5 (2010).
27. Polson, A.G. *et al.* Anti-CD22-MCC-DM1: an antibody-drug conjugate with a stable linker for the treatment of non-Hodgkin's lymphoma. *Leukemia* **24**, 1566-73 (2010).
28. Armitage, J.O. & Weisenburger, D.D. New approach to classifying non-Hodgkin's lymphomas: clinical features of the major histologic subtypes. Non-Hodgkin's Lymphoma Classification Project. *Journal of clinical oncology : official journal of the American Society of Clinical Oncology* **16**, 2780-95 (1998).
29. Skipper, H.E. & Perry, S. Kinetics of normal and leukemic leukocyte populations and relevance to chemotherapy. *Cancer research* **30**, 1883-97 (1970).
30. Brons, P.P. *et al.* Cell cycle kinetics in malignant lymphoma studied with in vivo iododeoxyuridine administration, nuclear Ki-67 staining, and flow cytometry. *Blood* **80**, 2336-43 (1992).
31. Frei, E., 3rd & Freireich, E.J. Progress and perspectives in the chemotherapy of acute leukemia. *Advances in chemotherapy* **2**, 269-98 (1965).
32. 0Holland, J.F. Clinical Studies of Unmaintained Remissions in Acute Lymphocytic Leukemia. In: *The Proliferation and Spreadof Neoplastic Cells* pp. 453-62. (The Williams& WilkinsCo, Baltimore, TheUniversity of Texas M. D. Anderson Hospital and Tumor Institute at Houston, 1968).
33. Tolo Diebkile, A. *et al.* Characteristics and Results of the Management of Diffuse Large B-Cell Lymphomas: The Experience of Cote d'Ivoire. *Advances in hematology* **2012**, 945138 (2012).
34. Gregory, W.M., Richards, M.A., Slevin, M.L. & Souhami, R.L. A mathematical model relating response durations to amount of subclinical resistant disease. *Cancer research* **51**, 1210-6 (1991).
35. Zhao, Y., Kosorok, M.R. & Zeng, D. Reinforcement learning design for cancer clinical trials. *Statistics in medicine* **28**, 3294-315 (2009).
36. Kantarjian, H. *et al.* Results of inotuzumab ozogamicin, a CD22 monoclonal antibody, in refractory and relapsed acute lymphocytic leukemia. *Cancer* **119**, 2728-36 (2013).
37. Cheson, B.D. *et al.* Revised response criteria for malignant lymphoma. *Journal of clinical oncology : official journal of the American Society of Clinical Oncology* **25**, 579-86 (2007).
38. Carnahan, J. *et al.* Epratuzumab, a humanized monoclonal antibody targeting CD22: characterization of in vitro properties. *Clinical cancer research : an official journal of the American Association for Cancer Research* **9**, 3982S-90S (2003).
39. Simeoni, M. *et al.* Predictive pharmacokinetic-pharmacodynamic modeling of tumor growth kinetics in xenograft models after administration of anticancer agents. *Cancer research* **64**, 1094-101 (2004).
40. Daniel J. DeAngelo, M.S., Giovanni Martinelli, Hagop Kantarjian, Michaela Liedtke, Wendy Stock, & Nicola Goekbuget, K.W., Luisa Pacagnella, Barbara Sleight, Erik Vandendries, Anjali S. Advani. EFFICACY AND SAFETY OF INOTUZUMAB OZOGAMICIN (INO) VS STANDARD OF CARE (SOC) IN SALVAGE 1 OR 2 PATIENTS WITH ACUTE LYMPHOBLASTIC LEUKEMIA (ALL): AN ONGOING GLOBAL PHASE 3 STUDY. In European Hematology Association.
41. Peterson, J.K. & Houghton, P.J. Integrating pharmacology and in vivo cancer models in preclinical and clinical drug development. *European journal of cancer* **40**, 837-44 (2004).

42. Kelland, L.R. Of mice and men: values and liabilities of the athymic nude mouse model in anticancer drug development. *European journal of cancer* **40**, 827-36 (2004).
43. Wong, H. *et al.* Antitumor activity of targeted and cytotoxic agents in murine subcutaneous tumor models correlates with clinical response. *Clinical cancer research : an official journal of the American Association for Cancer Research* **18**, 3846-55 (2012).
44. Kamb, A. What's wrong with our cancer models? *Nature reviews Drug discovery* **4**, 161-5 (2005).
45. Rocchetti, M., Simeoni, M., Pesenti, E., De Nicolao, G. & Poggesi, I. Predicting the active doses in humans from animal studies: a novel approach in oncology. *European journal of cancer* **43**, 1862-8 (2007).
46. Ducry, L. & Stump, B. Antibody-drug conjugates: linking cytotoxic payloads to monoclonal antibodies. *Bioconjugate chemistry* **21**, 5-13 (2010).
47. Agoram, B.M. & Demin, O. Integration not isolation: arguing the case for quantitative and systems pharmacology in drug discovery and development. *Drug Discov Today* **16**, 1031-6 (2011).
48. Shor, B., Gerber, H.P. & Sapra, P. Preclinical and clinical development of inotuzumab-ozogamicin in hematological malignancies. *Molecular immunology* **67**, 107-16 (2015).
49. Takeshita, A. *et al.* CMC-544 (inotuzumab ozogamicin) shows less effect on multidrug resistant cells: analyses in cell lines and cells from patients with B-cell chronic lymphocytic leukaemia and lymphoma. *British journal of haematology* **146**, 34-43 (2009).
50. Shah, D.K., Barletta, F., Betts, A. & Hansel, S. Key bioanalytical measurements for antibody-drug conjugate development: PK/PD modelers' perspective. *Bioanalysis* **5**, 989-92 (2013).
51. Okeley, N.M. *et al.* Intracellular activation of SGN-35, a potent anti-CD30 antibody-drug conjugate. *Clinical cancer research : an official journal of the American Association for Cancer Research* **16**, 888-97 (2010).
52. Thurber, G.M. & Dane Wittrup, K. A mechanistic compartmental model for total antibody uptake in tumors. *Journal of theoretical biology* **314**, 57-68 (2012).
53. Thurber, G.M., Schmidt, M.M. & Wittrup, K.D. Antibody tumor penetration: Transport opposed by systemic and antigen-mediated clearance. *Advanced Drug Delivery Reviews* **60**, 1421-34 (2008).
54. Minchinton, A.I. & Tannock, I.F. Drug penetration in solid tumours. *Nature reviews Cancer* **6**, 583-92 (2006).